

Population of ^{133}I from the beta decay of fission product $^{133}\text{Te}^g$ and the cluster-vibration model

H. G. Hicks, J. H. Landrum, E. A. Henry, and R. A. Meyer
Lawrence Livermore National Laboratory, Livermore, California 94550

S. Brandt and V. Paar

Zavod Za Teorijsku Fiziku, University of Zagreb, Zagreb, Croatia, Yugoslavia

(Received 27 August 1982; revised manuscript received 22 February 1983)

An automated rapid chemistry system has been used to isolate enriched sources of 12.4-min $^{133}\text{Te}^g$ from mixed fission products via the sequence $^{133}\text{Sb}(\beta)^{133}\text{Te}^g$. In addition, pure sources of $^{133}\text{Te}^g$ were obtained by using the reduction of Te^{VI} to Te^{IV} during the isomeric decay of $^{133}\text{Te}^m$. Singles, Compton suppression singles, and γ - γ coincidence Ge(Li) spectra were used to identify approximately 210 γ rays from the decay of $^{133}\text{Te}^g$. This information was used to establish 38 levels below 3000 keV in ^{133}I . Cluster-vibration model calculations have been carried out for the $Z=53$ nucleus ^{133}I . The calculated level structure and transition probabilities are found to be in good agreement with the experimental results.

[NUCLEAR STRUCTURE Cluster vibration model, energy levels, branching ratios.]
	RADIOACTIVITY $^{133}\text{Te}^g$ (from Autobatch chemical isolation from fission); measured E_γ , I_γ , γ - γ coin, Compton suppression; ^{133}I deduced levels J , π ; deduced β branch $\log ft$, HPGc and Ge(Li) detectors.	

I. INTRODUCTION

The cluster-vibration model (CVM) attempts to describe the low-energy excitations of odd-mass nuclei by coupling a dynamic cluster (particle clusters in a major shell) to the quadrupole vibrations of the underlying nuclear core.¹⁻⁸ The odd-mass iodine nuclei and their excitations provide the possibility of testing the CVM on a three-proton cluster ($Z=53$ iodine nuclei) interacting with varying degrees of quadrupole vibrational core softness from closed-shell ^{135}I to midneutron shell nuclei. In order to provide a full-range data base of detailed level properties for the iodine nuclei we have been studying the decay of tellurium isotopes and their population of odd-mass iodine nuclei. In previous papers^{9,10} we have presented data on ^{129}I and ^{131}I while earlier work of Apt and Walters gave detailed data for ^{127}I levels.¹¹ Subsequently, data will be given for the closed-shell ^{135}I nucleus.¹² Here we describe experiments which have used very rapid automated chemical techniques to produce enriched intense sources of $^{133}\text{Te}^g$. In companion presentations we discuss the high-spin negative parity states of ^{133}I populated in $^{133}\text{Te}^m$ decay¹³ and continuous chemistry (SISAK) studies which prove that the $(19/2)^-$ iso-

mer of ^{133}I is populated in 12% of all $^{133}\text{Te}^m$ beta decays.¹⁴⁻¹⁶

A very extensive detailed data base is necessary for the application of fission produce decay data to technical problems, such as the average amount of γ -ray and beta energy that must be compensated for following an unscheduled shutdown of a reactor, such as a loss-of-coolant accident.¹⁵ The input data needed to address such problems can be derived directly from a detailed knowledge of the decay scheme. In the present study we have determined an accurate decay scheme for $^{133}\text{Te}^g$. Previous work on this decay was last performed in 1968 by McIsaac,¹⁷ Parsa, Gordon, and Walters,¹⁸ and Berg, Fransson, and Bemis.¹⁹ These results have been compiled in Nuclear Data Sheets.²⁰

II. EXPERIMENTAL TECHNIQUES

Three separate experiments were performed in order to study the decay of $^{133}\text{Te}^g$. In the first series of experiments nonautomated techniques were used to isolate Te from fission products directly. The second series of experiments involve chemical separation of the ^{133}Te ground-state activity from the isomeric activity. The third set of experiments

made use of the Lawrence Livermore National Laboratory (LLNL) automated batch chemistry processor (Autobatch) system to provide high-intensity sources of enriched $^{133}\text{Te}^g$.

A. Nonautomated $^{133}\text{Te}^g$ separation

Sources of $^{133}\text{Te}^g$ were produced by isolating tellurium from mixed fission products produced in the irradiation of enriched ^{235}U with thermal neutrons at the LLNL Pool-Type Reactor (LPTR). The iodine activities were removed from the fission products followed by rapid isolation of the tellurium activities. These sources contained $^{129}\text{Te}^g$, $^{131}\text{Te}^g$, $^{133}\text{Te}^m$, and ^{134}Te in addition to the $^{133}\text{Te}^g$. Spectra were taken as a function of time in order to identify the $^{133}\text{Te}^g$ γ rays. Three energy ranges were used during measurements with Ge(Li) spectrometers: 0–1, 0–2, and 0–4 MeV. In the 0–4 MeV set of spectra two types of spectra were taken: one with no absorber and one with 12.7 mm of Pb absorber between the source and the Ge(Li) detector. For all these spectra a series of detectors was used, and an individual source was moved from detector to detector such that a single spectrometer observed a specific time period (equivalent to one half-life) after chemical separation from the mixed fission products. For each of the energy ranges the measurement was repeated with known γ -ray energy standard sources in place. In a separate experiment, thin sources were used to accumulate spectra in the range 0–400 keV with a LEPS spectrometer.

B. Separation of $^{133}\text{Te}^g$ from $^{133}\text{Te}^m$

The reduction of Te^{VI} to Te^{IV} during decay of the isomeric activity^{21,22} has been used to isolate $^{133}\text{Te}^g$ from $^{133}\text{Te}^m$ sources. This technique, described elsewhere,^{23,24} provides relatively pure $^{133}\text{Te}^g$ sources, albeit of low intensity. Our sequence of chemical isolation was first to isolate Te from mixed fission products; second, to allow the $^{133}\text{Te}^m$ present to decay by isomeric transition to $^{133}\text{Te}^g$; and third, to separate the $^{133}\text{Te}^g$, leaving the longer-lived $^{133}\text{Te}^m$ in solution for subsequent $^{133}\text{Te}^g$ isolations. Because of the low-intensity sources only large-volume Ge(Li) spectrometers were used, which enabled us to obtain the relative intensities of the more intense γ rays and identify them by half-life.

C. Enriched intense $^{133}\text{Te}^g$ sources from ^{133}Sb decay

The preceding experiments did not provide sources of sufficient intensity to study the γ rays of low abundance which were crucial to the full assessment of the $^{133}\text{Te}^g$ decay scheme.

The fission process produces directly many times

more $^{133}\text{Te}^m$ atoms than $^{133}\text{Te}^g$ atoms, effectively masking the low abundance γ rays associated with the ground state decay. However, 83% of all ^{133}Sb decays populate the ^{133}Te ground state. Therefore, the ratio of the disintegration rates of $^{133}\text{Te}^g$ to $^{133}\text{Te}^m$ in the daughter product of ^{133}Sb should initially be about a factor of 30 in favor of the ground state. The 2.8-min $^{132}\text{Sb}^m$ has about the same half-life as ^{133}Sb ; however, the 78-h $^{132}\text{Sb}^m$ daughter has such a low specific activity that there is no appreciable interference.

The chemical apparatus is discussed elsewhere^{15,16}; here we discuss the details of its operation for the separation of 12-min $^{133}\text{Te}^g$. First the noble gases, Kr and Xe, were purged from the fission product solution by a nitrogen stream. Addition of a solution of sodium borohydride generated the gaseous hydrides of As, Se, Sn, Sb, and Te.²³ The gas was passed through a 19 mm diam by 406 mm long Drierite trap that removed Te and Sn, through a 0.5 M NaOH trap that removed Se, and through a 6.4 mm diam by 51 mm long polyethylene tube containing glass wool wet with a saturated solution of KOH in methanol. As and Sb were trapped on the glass wool.^{15,16} The timing of each chemical step was as follows: 50 μg inactive Sb in 6 M HCl (3 ml) and the fission product solution (1 ml 0.5 N H_2SO_4) were drawn into the reaction vessel (0.31 s); the solution was purged with N_2 (1.60 s); 2 M NaBH_4 solution (~ 1 ml) was added (0.32 s); and the system was purged with N_2 (2.4 s). The time history of the automated experimental procedure is as follows:

End of irradiation:	~ 0.2 s
End of transit:	~ 2 s
End of chemistry:	~ 7.3 s
End of decay time to remove ^{134}Sb and As isotopes of mass ≥ 82 and transport of collection trap to counter:	40 s

After the ^{133}Sb had decayed for a period of 60 to 250 s, the $^{133}\text{Te}^g$ was isolated. The glass wool trap was washed with water into a boiling $(\text{NH}_4)_2\text{S}$ solution containing Te and Sb carriers. At the resumption of boiling a saturated solution of Na_2SO_3 was added dropwise until the solution turned black; then two more drops were added. The Te metal precipitate coagulated after boiling for about one minute. The resulting slurry was filtered through a millipore filter mounted in a chimney containing a mask to produce a source 6 mm in diameter. The precipitate was washed with water and acetone. Once dried, the source was sealed in plastic and placed in front of the spectrometer.

TABLE I. Energies, intensities, coincidence relationships, and assignments of the γ rays assigned to the decay of $^{133}\text{Te}^g$.

E_γ (ΔE_γ) (keV)	L_γ (ΔI_γ) (Relative)	Coincident γ rays	Assignment ^a		
			From	To	
67.22(—)	1.7(5)	407	786	719	
170.91(13)	1.5(5)		2768	2597	
183.3(4)	0.3(2)		2393	2210	
190.5(1)	0.9(4)	587,653,1061	1564	1373	
199.6(3)	0.6(2)		2225	2025	
207.4(1)	0.4(2)		2417	2210	
230.9(2)	0.3(1)		1564	1333	
242.0(1)	0.5(2)		2467	2225	
251.4(3)	0.5(2)		1564	1312	
302(1)	0.5(3)		2768	2467	
312.08(3)	1000 ^b	312,407,474,477,613,653, 914,844,927,930,995,1000, 1014,1021,1061,1252,1294, 1309,1359,1405,1473,1697, 1713,(1722),1824,1881, 1897,1912,1943,2081,(2180), 2213,2229,2263,2456,2496	312	g.s.	
324.3(2)	0.8(2)		1564	1239	
331.5(2)	1.9(7)		2541	2210	
338.22(2)	4.3(2)	312,(550?),1021,1333	1671	1333	
341(1)	0.5(2)		2808	2467	
343.9(1)	1.0(4)		1717	1373	
358.7(2)	1.4(2)	312,719,912,1000,1312	1671	1312	
368.9(2)	1.5(7)		2041	1671	
384.25(5)	4.4(5)	312,407,507,(546),786, 1021,1333	1717	1333	
392.44(3)	4.0(4)		1307	914	
394(1)	0.5(2)		1307	912	
404.85(7)	4.2(9)	312,1000,1312	1717	1312	
407.63(3)	434(5)	312,392,406,520,587 593,613,653,767,844, 951,986,993,997,1306, 1333,1416,(1473),1505, 1535,1564,(1773)	719	312	
410.40(6)	15(1)	312,394,407,719,587, 995,1307	1717	1307	
418.4(2)	0.4(1)		1333	914	
431.61(13)	2.0(5)		1671	1239	
452.9(1)	2(1)	312,460,474,544,190,	1239	786	
461.30(4)	10(2)	199,572,844,312,452,	2025	1564	
474.85(1)	14.1(5)	520,525,546,587,778, 884,930,1238,1266,1349, (1468),1680,(1706)	786	312	
477.77(6)	6.1(5)	312,927,1239	1717	1239	
485.0(2)	9.9(4)	9.0(4)			
484.5		0.9(4)	2768	2283	
488(2)	1.4(5)		2541	2053	
507.3(1)	2.2(3)	410,997	2225	1717	
520.10(1)	1.0		0.7(2)	1239	719
520.4(2)			0.3(2)	1307	786
525.84(3)	3.7(4)	312,474,786	1312	786	
543.5(5)	2(1)		2768	2225	

TABLE I. (Continued.)

E_γ (ΔE_γ) (keV)	L_γ (ΔI_γ) (Relative)	Coincident γ rays	Assignment ^a	
			From	To
546.29(3)	8.2(5)	312,474,786	1333	786
553.7(2)	1.0(4)	312,407,884	2225	1671
569.6(8)	0.9(2)		(1943)	1373)
572(1)	0.4(2)		2597	2025
586.71(4)	9.9(3)	312,474,786,	1373	786
587.6(4)	1.6(3)		1307	719
593.0(2)	2.8(5)	312,407,719	1312	719
613.52(3)	5.1(6)	312,338,384,407,719	1333	719
620(1)	0.5(2)	369,667	2661	2041
635.8(2)	1.1(4)			
645.6(1)	6.3(7)	407,844,(1252)	2210	1564
653.98(8)	5.0(6)	190,312,(343),407,718 762,851,910(653 + 1061 gate):190,312,343,407, 719,851,911,1224	1373	719
667(1)	3(1)		2041	1373
679.8(7)	1.0(5)		2053	1373
690.8(1)	2.2(5)	190,251,312,407,844	2255	1564
696(1)	1.3(7)			
702(1)	0.7(4)		2266	1564
712.6(5)	3(1)	198,312,407,(593?)	2025	1312
717.8(2)	1.8(8)	197,312,995	2025	1307
719.6	(≤ 1)		2283	1564
719.71(2)	142(8)	520,587,590,613,653, 844,951,997,1306,1333, 1416,1473,1489,1505, 1564,(1773)	719	g.s.
	144(8)			
720.3(5)	2(1)		2053	1333
722(1)	0.3(2)		2393	1671
727(1)	0.7(5)		2041	1312
740.8(2)	3.0(7)	312,1000	2053	1312
743.0(2)	5(1)	312,407,719,786,844 (1238)	2768	2025
745.8(2)	1.8(5)		2053	1307
762.8(2)	2.0(5)		2136	1373
778.0(3)	3.2(9)	312,474,786	1564	786
786.93(2)	86.5(1.5)	452,520,526,546,587 777,884,930,1238,1266, 1754	786	g.s.
802.9(3)	1.0(3)		1717	914
	3.1(3)			
803.3(3)	2.1(3)		2136	1333
813.4(2)	2.0(5)	312,927,1239	2053	1239
823.9(5)	1.3(4)		2136	1312
829.2(3)	1.5(4)	312,407,1307	2136	1307
844.36(1)	53(1)	312,407,(461),645,690, (702),719	1564	719
851.37(7)	5.0(6)	242,312,407,586,786, 1061	2225	1373
854.2(9)	1.0(5)		2525	1671
860.2(7)	1.0(5)		2193	1333
880.7(1)	1.0(5)		2193	1312
884.29(3)	11.6(9)	312,474,786,854,1137	1671	786

TABLE I. (Continued.)

E_γ (ΔE_γ) (keV)	L_γ (ΔI_γ) (Relative)	Coincident γ rays	Assignment ^a	
			From	To
886.0(4)	0.7(4)		2193	1307
888.9(4)	0.5(4)	312,407,450,675,719,	(1606	719)?
896.7(2)	0.8(2)		2136	1239
902.5(1)	3.0(5)	183,312,392,394,719, 912,914,956	2210	1307
910.0(7)			2283	1373
912.3(6)	4(2) {		2225	1312
912.69(2)	1.0(3)		912	g.s.
914.74(2)	1.0(6)	(171),392,418,802,1682	914	g.s.
922(1)	11(1)		2225	1333
926(1)	2(1)			
927.75(3)	3(1)			
	10.2(8) {	312,431,477,812,896, 1015,1123	1239	312
928(1)	2(1)		2493	1564
930.71(1)	61(2)	312,474,507,574,786,943	1717	786
934(1)	2(1)		2266	1333
942.2(2)	6(1) {	312,407,613,786,1000	2255	1312
943(1)	5(1)			
	1.0(7)		2661	1717
951.51(7)	3.6(6)		1671	719
971(1)	0.8(5)		2283	1312
978(1)	2(1)	312,407,478,573,778,844	2541	1564
995.09(2)	11.1(8)	312,410,719,745,829,886	1307	312
997.66(1)	16.6(8)	312,407,477,719	1717	719
1000.72(1)	58(1)	251,312,404,712,740, 823,880,912,942,1455	1312	312
1015.3(3)	2.0(7)		2255	1239
1021.13(8)	45(1)	312,384,922	1333	312
1026.8(2)	0.9(3)		2266	1239
1051.1(3)	0.8(3)		2363	1312
1061.61(1)	19(2)	312,667,679,762,851, 1224	1373	312
1109.9(2)	2(1)		2417	1307
1123.9(3)	1.0(7)		2363	1239
1137(1)	2(1)		2808	1671
1156.3(3)	1.1(4)		(1943	786)?
1208.5(3)	2.6(6)		2541	1333
1221.7(3)	0.3(1)		2136	914
1224(1)	0.10(5)		2597	1373
1227.7(4)	1.8(3)		2467	1239
1238.5(5)	5.3(8) {	312,477,787 813	2025	786
	2(1)			
1239.9(3)	3.3(8)		1239	g.s.
1243.9(2)	1.2(4)		2808	1564
1252.08(2)	23(1)	312	1564	312
1254.2(5)	0.3(1)		2041	786
1266.58(5)	3.1(6)	312,474,786	2053	786
1285(1)	0.8 {		2597	1312
1286(1)	0.4(2)		2525	1239
1290(1)	0.4(2)		2597	1307
1290(1)	0.3(2)			
1294.0(2)	2.3(4)			
1302(1)	0.7(4)		2541	1239

TABLE I. (Continued.)

E_γ (ΔE_γ) (keV)	L_γ (ΔI_γ) (Relative)	Coincident γ rays	Assignment ^a		
			From	To	
1306.0(6)	12.9(4)	{ 4.3(5)	2025	719	
1307.2(2)			1307	g.s.	
1310.4(12)			2225	914	
1312.80(23)		13.7(7) 404,712	1312	g.s.	
1320.4(6)		0.4(2) 312,407,720	2041	719	
1333.21(2)	172(3)	{ 171(3)	230,311,338	1333	g.s.
1333.7(5)			384,407,553,720		
			804	2053	719
1349.63(13)		1.6(5)	2136	786	
1359.45(7)		1.5(3) 312,553,722	1671	312	
1371.7(5)		0.16(7)	2935	1564	
1405.48(52)		9.4(8)	1717	312	
1416.90(7)		2.1(4)	2136	719	
1438(1)		0.1(1)	2225	787	
1455.24(7)		2.4(9)	2768	1312	
1468.2(6)		0.8(5)	2255	786	
1473.74(8)		5.1(5)	2193	719	
1489.88(14)		1.9(4)	2210	719	
1493(1)		0.4(2)	2866	1373	
1502.8(5)		0.5(4)	2417	914	
1505.2(3)		1.1(5)	2225	719	
1535.1(1)		3.4(5)	2255	719	
1564.0(2)		1.2(3)	2283	719	
1630.1(3)		0.4(2)	2417	786	
1633.7(2)		1.2(3)	(1945	312)	
1671.19(7)		2.6(4)	1671	g.s.	
1680(1)		1.5(9)	2467	786	
1682.9(2)		2.2(4)	2597	914	
1697.3(2)		1.0(4)	2417	719	
1706(1)		1.0(7)	2493	786	
1713.0(5)		6(1)	2025	312	
1717.61(1)		51(2)	1717	g.s.	
1722(1)		1.3(5)	(2034	312)	
1738(2)		0.8(4)	2525	786	
1741.57(8)		2.2(2)	2053	312	
1754.9(2)		0.7(1)	2541	786	
1773.27(7)		2.2(7)	2494	719	
1806.9(1)		4.1(4)	2525	719	
1821.7(2)		3.5(4)	2541	719	
1824.25(3)		6.4(5)	2136	312	
1881.52(4)		19.5(7)	2193	312	
1893.21(22)		0.9(3)	(2205	312)	
1897.59(7)		1.7(1)	2210	312	
1912.91(6)		1.9(1)	2225	312	
1938(1)		0.5(3)	(2246	312)	
1943.8(1)		1.3(2)	2255	312	
1972(2)		0.24(8)	(2283	312)	
2025.6(2)		1.3(2)	2025	g.s.	
2036.2(3)		0.3(1)			
2048.5(4)		0.6(2)	2768	719	
2053.43(8)		2.3(5)	2053	g.s.	
2079.3(2)		1.5(3)	2866	786	
2081.3(3)		0.9(3)	2393	312	

TABLE I. (Continued.)

E_γ (ΔE_γ) (keV)	L_γ (ΔI_γ) (Relative)	Coincident γ rays	Assignment ^a	
			From	To
2093(1)	0.3(2)			
2105.5(2)	1.6(4) ^c		2417 ^c	312 ^c
2136.51(8)	20(1)		2136	g.s.
2148.3(4)	0.4(2)		2935	786
2155(1)	0.4(3)		2467	312
2180.9(4)	0.5(3)		2492	312
2193.65(5)	9.1(7)		2193	g.s.
2210.22(4)	11(1)		2210	g.s.
2213.6(1)	3.4(6)		2525	312
2225.00(14)	3.6(4)		2225	g.s.
2229.64(3)	14(1)		2541	312
2255.4(1)	3.3(5)		2255	g.s.
2266.4(1)	3.8(5)		2266	g.s.
2285.5(4)	0.15(5)		2597	312
2336(1)	0.23(9)			
2349(1)	0.13(7)		2661	312
2363(1)	0.4(2)		2363	g.s.
2393(1)	0.2(1)		2393	g.s.
2417.7(1)	3(1)		2417	g.s.
2456.20(9)	4.1(4)		2768	312
2467.40(7)	6.5(5)		2467	g.s.
2485(1)	0.3(2)			
2496.35(12)	3.1(4)		2808	312
2525.5(4)	0.4(2)		2525	g.s.
2541.80(7)	8(1)		2541	g.s.
2554.19(7)	5.6(6)		2866	312
2597.7(3)	0.9(3)		2597	g.s.
2623.82(16)	1.5(3)		2936	312
2661.1(4)	1.2(3)		2661	g.s.
2825.30(14)	2.5(3)		2825	g.s.

^aLevels in parentheses are only tentatively proposed. They are not included in the decay scheme.

^bThis is the fiducial γ ray. Its error is the statistical plus peak-shape fitting error of the photo-peak which, in this case, was 0.3%.

^cAlternate placement is the transition between the 2825- and 719-keV levels.

Gamma-ray spectra in the energy range 0–4000 keV were measured from these $^{133}\text{Te}^g$ sources with a 8192 channel Ge(Li) spectrometer. In one series there was 25.4 mm of Pb absorber between the source and detector. These measurements were repeated several times varying only the time of separation of Te from Sb. In all these measurements a freshly-separated source replaced the old source every 15 min. A similar schedule of source replacement was used to measure the γ - γ coincidence spectra with the LLNL megachannel spectrometer.

All spectra were analyzed on the LLNL CDC 7600 computer network using the data reduction code GAMANAL. Initial analysis of the γ - γ coincidence data was performed on-line using the megachannel analyzer.

III. RESULTS AND DECAY SCHEME

In Table I we present the results of our experiments. In the table we list the γ -ray energies as calibrated against known standards²⁵ based on the 411-keV Au line having a value of 411.80441 keV. The table lists the relative γ -ray intensities which can be converted into absolute γ -ray intensities per 1000 decays by multiplying by the factor 0.622. This factor was derived from the detailed balance technique, assuming a negligible ground-state-to-ground-state beta transition [$^{133}\text{Te}(3/2)^+$ to $^{133}\text{I}(7/2)^+$] and pure M1 multipolarity for the 312-keV γ ray.

The decay scheme for $^{133}\text{Te}^g$ is shown in Figs. 1(a)–(h) while in Table II we present the percent beta feeding to individual levels. The $\log ft$ values

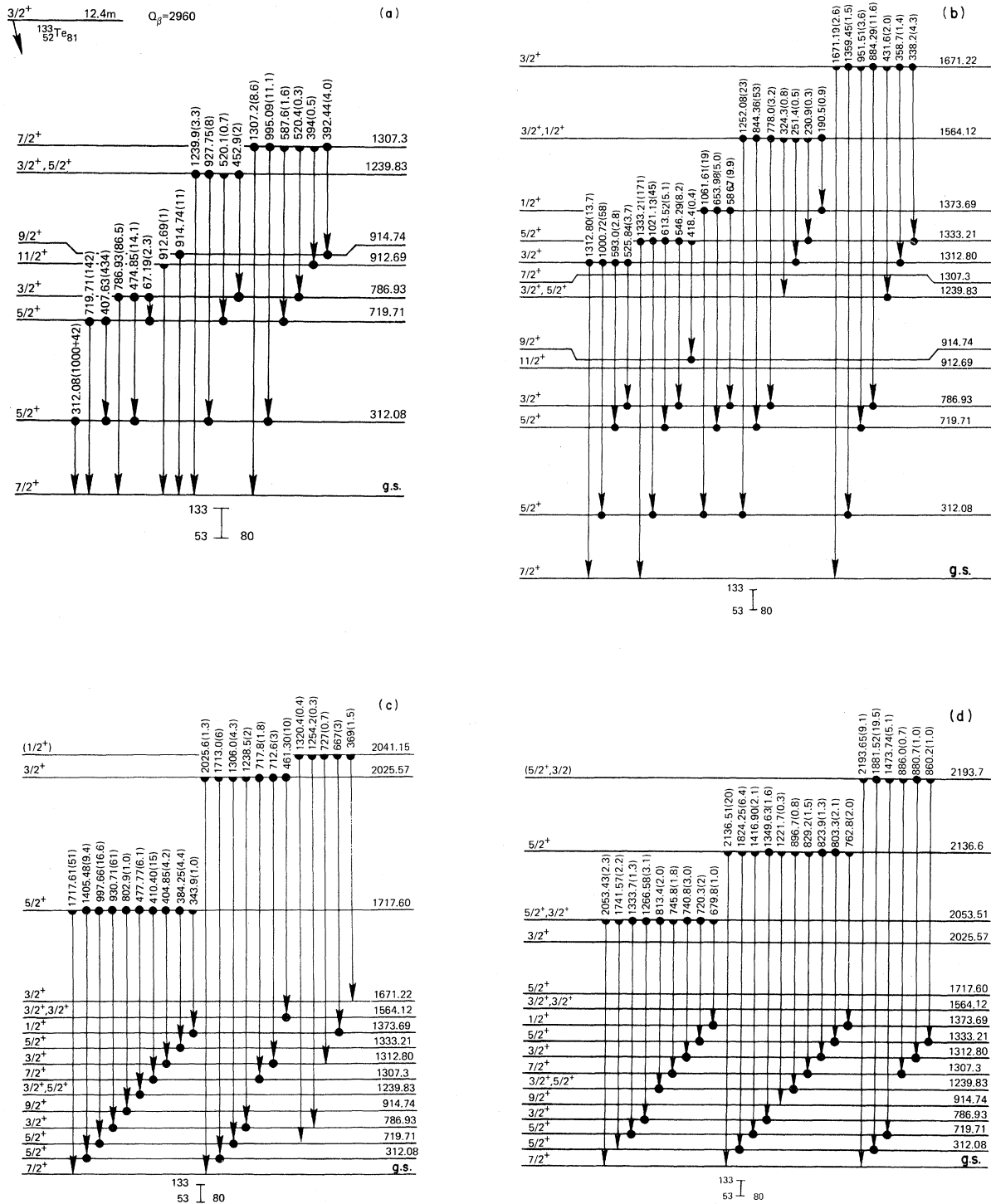


FIG. 1. Decay scheme for the decay of $^{133}\text{Te}^g$ to levels of ^{133}I . Full circles at the bottom of the arrow signify replacement of the γ ray by observation in at least one gated γ ray, while a full circle at the top of the arrow signifies that a gate was set for that γ ray. Half circles at the top of the arrow signify no gate was set but that placement is confirmed by the Ritz principle. (a) levels up to 1310 keV; (b) from 1310 to 1675 keV; (c) from 1700 to 2050 keV; (d) from 2050 to 2200 keV; (e) from 2200 to 2270 keV; (f) from 2270 to 2530 keV; (g) from 2530 to 2700 keV; and (h) above 2700 keV.

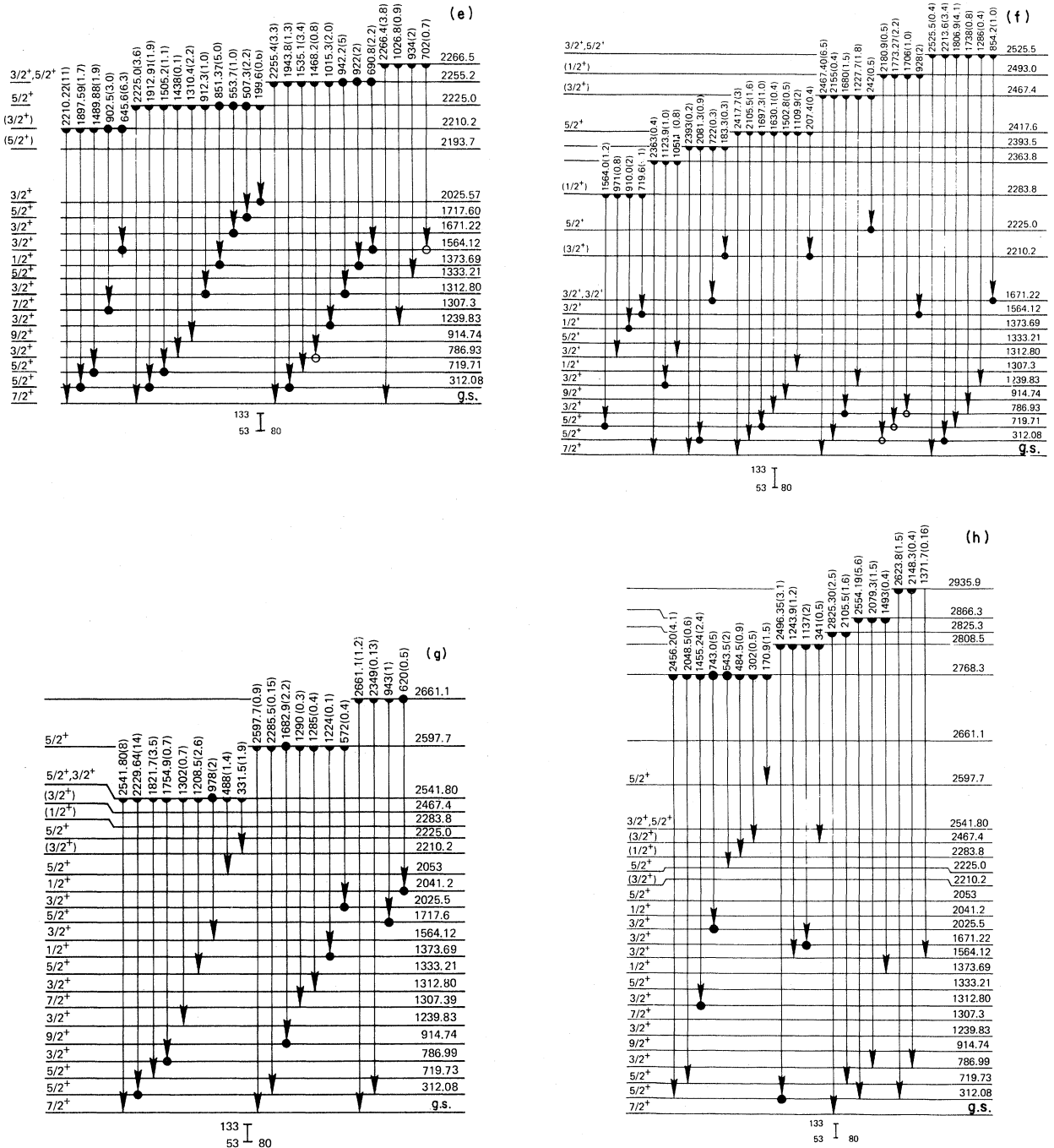


FIG. 1. (Continued.)

listed in Table II are obtained by using a half-life of 12.4 m and a decay energy of 2960 ± 100 keV.²⁰ Also listed in the last column of Table II are the most consistent values for J^π of the levels. The J^π assignments of levels below 1000 keV have been discussed elsewhere, as noted in Table II. An unambiguous assignment cannot be given for levels above 2600 keV because the error in the Q value allows too

wide a range of $\log ft$ values.

IV. DISCUSSION

Here we describe the ¹³³I nucleus within the framework of the cluster-vibration model (CVM).^{1-3,26-28} In the CVM, a dynamical cluster consisting of three proton particles in the 50-82

TABLE II. Percent beta feeding, $\log ft$ value, and J^π values for levels of ^{133}I .

Level (keV)	Beta feeding (per 100 decays)	$\log ft$	Preferred J^π /comment
0			7/2 ⁺ Assigned in NDS
312	21.3	6.70	5/2 ⁺ Assigned in NDS
719	28.3	6.29	5/2 ⁺ Proposed by Parsa <i>et al.</i>
787	(< 1)	(> 8)	3/2 ⁺ Proposed by Parsa <i>et al.</i>
912			11/2 ⁺ Proposed by Holm
914			9/2 ⁺ Proposed in isomer decay work
1239	0.5	8.8	3/2 ⁺ , 5/2 ⁺ a,b
1307			7/2 ⁺ c, proposed in isomer decay work
1312	52.6	6.68	3/2 ⁺ a,b
1333	13.0	6.07	5/2 ⁺ a,b
1373	1.0	7.1	1/2 ⁺ a,d
1564	3.5	6.4	1/2 ⁺ , 3/2 ⁺ a,d
1671	1.3	6.7	3/2 ⁺ a,b
1717	10.0	5.7	5/2 ⁺ a,e
2025	1.2	6.2	3/2 ⁺ a,b
2041	0.34	6.7	(1/2 ⁺) a,(b)
2053	1.1	6.2	5/2 ⁺ , 3/2 ⁺ a,b
2136	2.4	5.7	5/2 ⁺ a,e
2193	2.3	5.6	(5/2 ⁺ , 3/2 ⁺) a,f
2210	1.3	5.8	(3/2 ⁺ , 5/2 ⁺) a,f
2225	1.2	5.8	5/2 ⁺ a,e
2255	1.2	5.7	3/2, 5/2 a
2266	0.5	6.2	h a
2283	0.2	6.5	h a
2363	0.14	6.5	h a
2393	0.10	6.5	h a
2417	0.55	5.7	5/2 ⁺ a,e
2467	0.60	5.5	(3/2 ⁺) a,f
2492	0.35	5.7	(1/2 ⁺) a,f
2525	0.57	5.4	3/2 ⁺ , 5/2 ⁺ a,b
2541	2.12	4.7	5/2 ⁺ , 3/2 ⁺ a,b
2597	0.19	5.6	5/2 ⁺ a,e
2661	0.14	g	g
2768	0.93	g	g
2808	0.42	g	g
2825	0.25	g	g
2866	0.46	g	g
2935	0.13	g	g

^aPopulated in beta decay, therefore $1/2 \leq J \leq 5/2$.

^b γ -ray branching consistent with this assignment.

^cPopulates 11/2⁺ level and 3/2⁺ level.

^dPopulates levels of $J^\pi \leq 5/2^+$.

^ePopulates levels of J^π up to 9/2⁺.

^fCriteria for J^π selection are only marginally met.

^gThe Q_β value is 2960 keV with an error of 100 keV. Because of the wide variation in possible $\log ft$ value that results, no value is quoted for levels with an energy larger than 2600 keV.

^hNo preferred value is given (insufficient information is available).

shell is coupled to the core quadrupole vibration. Other iodine isotopes have been discussed within the framework of the CVM using a three-proton cluster,^{2,27} and even Te isotopes have been described us-

ing a two-proton cluster.⁴⁻⁶ The interplay of a dynamical few-particle shell-model cluster and a vibrational degree of freedom generally gives rise to the coexistence of vibrationlike, rotationlike, and

TABLE III. Comparison of the experimental and calculated branching ratios in ^{133}I . The calculated transitions from each state are normalized to the corresponding experimental transition with strongest intensity.

I	Level (keV)	Transition		E_γ (keV)	I_γ (exp)	Identification	$B(E2)$ (e^2b^2)	$B(M1)$ (μ_N^2)	I_γ (th)	Alternative identification	I_γ (th)
7/2						7/2 ₁					
5/2	312	2	1	312	1000	5/2 ₁	0.0326	0.0187	1000		
5/2	720	3	1	720	142	5/2 ₂	0.0766	0.0033	396		
		3	2	408	434		0.0003	0.1854	434		
3/2	787	4	1	787	87	3/2 ₁	0.1085	0	87		
		4	2	475	14		0.0162	0.1260	53		
11/2	913	5	1	913	1.0	11/2 ₁	0.0852	0	1.0		
9/2	915	6	1	915	11	9/2 ₁	0.0575	0.0050	11		
		6	2	603	<0.4		0.0113	0	0.2		
		7	1	1240	3.3		0.0053	0	0.8		1.3
3/2	1240	7	2	928	8.0	3/2 ₂	0.0026	0.1421	8.0	5/2 ₃	8.0
(5/2)		7	3	520	0.7		0.0451	0.0432	0.5		0.5
		7	4	453	2		0.0509	0.0015	0.1		0.2
		8	1	1307	9		0.0036	0.0091	4		
7/2	1307	8	2	995	11	7/2 ₂	0.0717	0.0396	11		
		8	5	395	0.5		0.0016	0	0.001		
		8	6	392	4		0.0159	0.0910	1		
		9	1	1313	14		0.0019	0	1		5
3/2	1313	9	2	1001	58	3/2 ₃	0.0397	0.2605	58	3/2 ₂	58
		9	3	593	3		0.0085	0.1055	4		4
		9	4	0.526	4		0.0003	0.0037	0.1		0.6
		10	1	1.333	171		0.0013	0.0011	171		171
		10	2	1.021	45		0.0453	0.0110	1250		6100
5/2	1333	10	3	0.613	5	5/2 ₃	0.0037	0.0125	83		78
		10	4	0.546	8		0.00004	0.0078	34		
		10	6	0.418	0.4		0.0043	0	1.0		0.4
1/2	1374	11	2	1.061	19	1/2 ₁	0.1104	0	19	1/2 ₂	19
		11	3	0.654	5		0.0243	0	0.4	(Note a)	35

^aThe experimentally-observed 1564-keV level has a branching ratio of 19–44, which is consistent with the 19–35 ratio predicted here for the (1/2)₂ branching ratio.

^b1/2₂.

It is interesting to compare the above six lowest-lying positive-parity states in ^{133}I with the six lowest-lying positive-parity states in the $^{95}\text{Mo}_{53}$ nucleus.²⁶ In the case of ^{133}I , the three-proton cluster with $j = g_{7/2}$ is the lowest state. In both cases the lowest-lying doublet $I = j, j - 1$ is followed by a quadruplet consisting of the states $I = j - 2, j - 1, j + 1, j + 2$ of about 0.2-MeV splitting. This is a consequence of the close resemblance between the

recouplings appearing in the matrix elements of the Hamiltonian for $J \geq (5/2)$.

The electromagnetic properties of level deexcitation were described by using the calculated wave functions. The effective charges and gyromagnetic ratios are as follows: $e^{\text{SP}} = 1.5$, $e^{\text{vib}} = 2.5$, $g_R = Z/A$, $g_I = g_I^{\text{free}} = 1$, $g_S = 0.7g_S^{\text{free}} = 3.91$. The polarization charge employed here (0.5) is the same as that used in the calculation for $^{95}\text{Mo}_{53}$ (Ref. 26) and nuclei in

the other regions of the Periodic Table; it corresponds approximately to the value used for doubly-closed shell nuclei. The effective vibrational charge $e^{\text{vib}}=2.5$ is typical of the $Z=50-82$ region.^{2,3} The relation between the effective and free gyromagnetic ratios employed is the one used in other cluster-vibration calculations for the 50-82 valence shell. In the present calculation we also include the tensor term in the $M1$ operator

$$\vec{M}_T(M1) = \left[\frac{3}{4\pi} \right]^{1/2} g_p(Y_2 \times s)_1,$$

which incorporates the effects of the 1^+ core polarization and of the mesonic exchange current.^{7,30,31} The gyromagnetic ratio g_p was chosen in accordance with Refs. 7 and 30: $g_p = \frac{1}{100}$ and $g_s^{\text{free}} \langle r^2 \rangle = 1.26$. Thus, no adjustment to ^{133}I was performed.

The static quadrupole moments of the ground state calculated in this way are

$$Q(7/2)_1^+ = -0.29 \text{ e b},$$

$$\mu(7/2)_1^+ = 2.2 \mu_N,$$

while the corresponding experimental values are -0.27 e b and $2.8 \mu_N$, respectively.

The calculated $B(E2)$ and $B(M1)$ values between positive-parity states are presented in Table III. The calculated branching ratios are compared with the experimental ones; results for two alternative identifications of levels are given in a few cases only. In

all other cases presented in the table the strongest transition of each branch is predicted correctly except for the 1.333 MeV $(5/2)^+$ level.

The $(1/2)^+$ levels in the iodine nuclei deserve mention because of their distinguishing features, in particular, their more rapid decrease in energy relative to other levels as neutron pairs are removed beyond shell closure, as shown in Fig. 2. The major components of these levels consist of the $d_{5/2}$ cluster, its interaction with the vibrational core, and the $s_{1/2}$ strength admixed through the non-spin-flip matrix elements. It may well be the latter that provides the rapid descent of the $1/2^+$ level in these nuclei because such $J-2$ states, resulting from mixing the $|d_{5/2}2_1^+\rangle$ component with $|s_{1/2}0_1^+\rangle$ by the non-spin-flip matrix element, are more strongly affected by the softening vibrational core.³²

ACKNOWLEDGMENTS

The authors wish to thank Dr. C. Gatrousis for his support of this work. The technical assistance of Dr. W. Ruhter as well as that of O. G. Lien and K. Mathews is appreciated. The partial support of the Department of Energy-Basic Energy Sciences Division to perform studies of decay-heat isotopes at LLNL is gratefully acknowledged. This work was performed under the auspices of the U.S. Department of Energy by the Lawrence Livermore National Laboratory under contract number W-7405-ENG-48.

¹G. Alaga and G. Ialongo, Nucl. Phys. **A97**, 600 (1967).
²V. Paar, Phys. Lett. **39B**, 466 (1972); **39B**, 587 (1972); **42B**, 8 (1972); Nucl. Phys. **A211**, 29 (1973); Phys. Rev. C **11**, 1432 (1975).
³V. Paar and B. K. S. Koene, Z. Phys. A **279**, 203 (1976); V. Paar, U. Eberth, and J. Eberth, Phys. Rev. C **13**, 2532 (1976); V. Paar, Ch. Vieu, and J. S. Dionisio, Nucl. Phys. **A284**, 199 (1977).
⁴V. Lopac, Nucl. Phys. **A155**, 513 (1970).
⁵G. Alaga, V. Paar, and V. Lopac, Phys. Lett. **43B**, 459 (1973).
⁶V. Paar (unpublished).
⁷V. Paar and S. Brandt, Phys. Lett. B **74**, 297 (1978).
⁸V. Paar and S. Brandt, Nucl. Phys. A **303**, 96 (1978).
⁹L. G. Mann, W. B. Walters, and R. A. Meyer, Phys. Rev. C **14**, 1141 (1976).
¹⁰S. V. Jackson, W. B. Walters, and R. A. Meyer, Phys. Rev. C **11**, 1323 (1975).
¹¹K. Apt and W. B. Walters, Phys. Rev. C **9**, 310 (1974).

¹²O. G. Lien III, E. A. Henry, and R. A. Meyer (unpublished).
¹³W. B. Walters and R. A. Meyer, Phys. Rev. C (to be published).
¹⁴H. C. Griffin, K. G. Skarnemark, and R. A. Meyer, Z. Phys. (to be published).
¹⁵R. A. Meyer, *Rapid Automated Nuclear Chemistry in Nuclear Spectroscopy of Fission Products*, edited by T. von Egidy (Institute of Physics, Bristol, 1979).
¹⁶R. A. Meyer, E. A. Henry, O. G. Lien III, H. C. Griffin, S. M. Lane, R. P. Yaffe, P. C. Stevenson, and G. Skarnemark, in *Proceedings of the Conference on Future Directions in Studies of Nuclei far from Stability, Nashville, Tennessee*, edited by J. H. Hamilton, E. H. Spejwsky, C. R. Bingham, and E. F. Zganjar (North-Holland, Amsterdam, 1980).
¹⁷L. D. McIsaac, Phys. Rev. **172**, 1253 (1968).
¹⁸B. Parsa, G. E. Gordon, and W. B. Walters, Nucl. Phys. **A110**, 674 (1968).

- ¹⁹I. Berg, G. Fransson, and C. Bemis, *Ark. Fys.* 37, 213 (1968).
- ²⁰E. A. Henry, *Nucl. Data Sheets* 11, 495 (1974).
- ²¹S. G. Prussin and W. W. Meinke, *Radiochim. Acta* 4, 79 (1965).
- ²²R. R. Williams, Jr., *J. Chem. Phys.* 16, 513 (1948).
- ²³A. E. Greendale and D. L. Love, *Anal. Chem.* 35, 632 (1963).
- ²⁴R. L. Hahn, *J. Chem. Phys.* 39, 3482 (1963).
- ²⁵R. A. Meyer, Lawrence Livermore Laboratory Report M-100, 1978 (unpublished).
- ²⁶R. A. Meyer, K. V. Marsh, D. S. Brenner, and V. Paar, *Phys. Rev. C* 16, 417 (1977).
- ²⁷R. Almar, O. Civitarese, F. Krmpotić, and J. Navara, *Phys. Rev. C* 6, 187 (1972); A. Szanto de Toledo, M. N. Rao, O. Sala, and F. Krmpotić, *ibid.* 16, 438 (1977).
- ²⁸G. Vanden Berghe, *Z. Phys.* 266, 139 (1974).
- ²⁹E. Browne and J. M. Dairiki, in *Table of Isotopes*, 7th ed., edited by C. M. Lederer and V. S. Shirley (Wiley, New York, 1978).
- ³⁰I. Hamamoto, *Phys. Lett.* 61B, 343 (1976).
- ³¹A. Arima, *J. Phys. Soc. Jpn.* 34, 205 (1973).
- ³²V. Paar and R. A. Meyer (unpublished).